

# Mimicking the Bird Flocking Behavior for Controlling Congestion in Sensor Networks

Pavlos Antoniou and Andreas Pitsillides  
Department of Computer Science  
University of Cyprus  
Nicosia, Cyprus  
Email: paul.antoniou@cs.ucy.ac.cy,  
andreas.pitsillides@cs.ucy.ac.cy

Andries Engelbrecht  
Department of Computer Science  
University of Pretoria,  
Pretoria, South Africa,  
Email: engel@cs.up.ac.za

Tim Blackwell  
Department of Computing  
Goldsmiths College  
University of London, UK  
Email: tim.blackwell@gold.ac.uk

**Abstract**—This study deals with the problem of congestion in wireless sensor networks (WSNs) and proposes a robust and self-adaptable nature-inspired congestion control approach for real-time event-based applications. WSNs face important limitations in terms of energy, memory and computational power. The uncontrolled use of limited resources in conjunction with the unpredictable nature of WSNs in terms of traffic load injection, wireless channel capacity fluctuations and topology modifications (e.g. due to node failures) may lead to congestion. Inspiration is drawn from the flocking and obstacle avoidance behavior of birds to ‘guide’ packets bypass obstacles like congestion regions and dead node zones. Recent studies showed that the flock-based congestion control (Flock-CC) approach is robust, self-adaptable and energy-efficient, involving minimal information exchange and computational burden when used in uniform grid topologies. The applicability of the Flock-CC in random topologies is investigated in this paper. Performance evaluations showed that Flock-CC was able to both alleviate congestion and minimize energy tax. Also, Flock-CC demonstrated robustness against failing nodes, and outperformed other congestion-aware routing approaches in terms of packet delivery ratio, end-to-end delay and energy tax.

## I. INTRODUCTION

In recent years, there has been an unprecedented research interest in the area of Wireless Sensor Network (WSNs). WSNs comprise of small (and often cheap), cooperative devices (nodes) which may be constrained in terms of computation capability, memory space, communication bandwidth and energy supply. Sensor nodes are envisioned to operate autonomously without external intervention and may interact (a) with the environment so as to sense or control physical parameters, and (b) with each other in order to exchange information or forward data towards one or more sink nodes. This mass of interactions, in conjunction with variable wireless network conditions, may result in unpredictable behavior in terms of traffic load variations and link capacity fluctuations. The problem is worsened due to topology changes driven by node failures, mobility, or intentional misbehavior. These stressful situations are likely to occur in WSN environments, thus increasing their susceptibility to congestion.

This paper proposes a *robust and self-adaptable nature-inspired congestion control (CC) mechanism* for real-time event-based WSNs. The proposed approach mimics the *flock-*

*ing behavior of birds*, where packets are modeled as birds flying over a topological space (sensor network). The packets are generated by sensor nodes and are ‘guided’ to form flocks and ‘fly’ towards a global attractor (sink), whilst trying to avoid obstacles (congested regions). The direction of motion is influenced by (a) repulsion and attraction forces exercised by neighboring packets, as well as (b) the gravitational force in the direction of the sink. The flock-based congestion control (Flock-CC) approach provides congestion detection on the basis of node and channel loading and traffic redirection over multiple paths. Flock-CC was initially proposed in [1] and with slight modifications in [2], [3] and [4]. These studies evaluated the Flock-CC approach in a uniform grid topology and the results showed that Flock-CC achieves low packet loss resulting in high packet delivery ratio (PDR) and thus reliability, low latency, fault tolerance, and low energy consumption. Flock-CC was also found to outperform congestion-aware multi-path routing approaches. This paper evaluates the Flock-CC approach in more realistic sensor network scenarios, where the positions of the nodes are random.

The rest of this paper is organized as follows: Section II deals with different aspects of congestion in WSNs. Section III presents the proposed flock-based approach. Section IV presents performance evaluation results. Section V draws conclusions and proposes areas of future work.

## II. CONGESTION IN WSNs

This section covers the problem of congestion in WSNs, refers to the symptoms and the consequences of congestion, and presents a number of recent CC approaches.

### A. The problem

Congestion occurs when the traffic load injected into the network exceeds available capacity at any point of the network. Typically, WSNs operate under light load but large, sudden, and correlated-synchronized impulses of packets may suddenly arise in response to a detected or monitored event. All packets must be directed towards one or more sink nodes. Large number of generated packets as well as the uncontrolled use of scarce network resources may lead to congestion.

## B. Types of congestion

In WSNs, there are mainly two types of congestion phenomena:

- 1) **Node-based:** When the incoming traffic load exceeds the outgoing channel capacity at a particular node, packets are being accumulated in the node's buffer. If the problem persists, instantaneous queue length exceeds the buffer capacity leading to buffer overflow, and long delays.
- 2) **Link-based:** The multi-hop nature of WSNs, the shared communication medium and the limited bandwidth give rise to link-based congestion. In wireless networks, local channel contention arises in the vicinity of a sensor node due to the limited bandwidth and interference among multiple neighboring nodes that try to access the wireless medium simultaneously. As a result, the time-variant nature of the outgoing channel capacity makes the congestion level fluctuating and unpredictable. The problem is worsened in densely deployed topologies.

## C. Symptoms of congestion

In traditional Internet wired networks, buffer drops are taken as an indication of congestion, while congestion control is usually carried out in an end-to-end manner (i.e. only the source-destination pair is involved). End-to-end CC approaches will not be effective in such error prone environments because the end-to-end nature may result in reduced responsiveness causing increased latency and high error rates, especially during long periods of congestion. Furthermore, simulation studies conducted by [5] and [6] revealed that, in WSNs where the wireless medium is shared using Carrier Sense Multiple Access (CSMA)-like protocols, wireless channel contention losses can dominate buffer drops and increase quickly with offered load. The problem of channel losses is worsened around hot spot areas, as for example, in the proximity of an event, or around the sink. In the former case, congestion occurs if many nodes report the same event concurrently, while in the latter case congestion is experienced due to the converging (many-to-one) nature of packets from multiple sending nodes to a single sink node. These phenomena result in the starvation of channel capacity in the vicinity of senders, while the wireless medium capacity can reach its upper limit faster than queue occupancy [7]. Thus, queue occupancy alone cannot accurately serve as an indication of congestion. Also, due to their severely constrained nature, WSNs necessitate autonomous, decentralized CC strategies which promise fast, effective and efficient relief from congestion. Decentralized approaches are expected to adopt a hop-by-hop model where all nodes along a network path can be involved in the procedure. Each node should make decisions based only on locally available information (e.g. buffer load, channel load) since none of them has complete information about the system state.

## D. Consequences

Congestion causes energy waste, throughput reduction, increase in collisions and retransmissions at the MAC layer,

increase of queuing delays and even information loss, leading to the deterioration of the offered quality of service (QoS), decrease of network lifetime and even the decomposition of network topology in multiple components.

## E. Related work

Various CC approaches can be found in WSNs literature based on traffic manipulation (e.g. rate adaptation to network changes [5], [6], multi-path routing [8]), topology control (e.g. clustering formation [9]), and network resource management (e.g. power control, multiple radio interfaces [10]). The majority of CC approaches are based on rate control that alleviates congestion by throttling the injection of traffic in the network. However, rate control attempts to decrease the reporting rate of nodes during (transient or persistent) congestion phenomena and may result in the deterioration of the offered quality of service, perhaps when needed the most. Furthermore, clustering formation assumes special roles in the network (e.g. clusterheads), while additional mechanisms are needed for maintaining and re-assigning roles. Also, areas around clusterheads may progressively become collision hot spots. Congestion mitigation based on power control and multiple radio interfaces seems unrealistic in WSNs since the low-cost nodes incentive is violated. On the other hand, multi-path routing has potential to effectively and efficiently alleviate congestion without deteriorating the offered network QoS. TADR [8] constructs a mixed potential field using depth and normalized queue length to route packets around the congestion areas and scatter the excessive packets along multiple paths consisting of idle and under-loaded nodes. However, the dynamic conditions of the wireless medium which may cause excessive packet loss in WSNs are not considered since a perfect (but practically infeasible) MAC protocol is assumed that provides a stable radio link without causing collisions.

## III. THE FLOCK-BASED CONGESTION CONTROL APPROACH

The main idea of the proposed Flock-CC model is to 'guide' packets to form groups or flocks, and flow towards a global attractor (sink), whilst trying to avoid obstacles (congestion regions) as illustrated in Fig. 1.

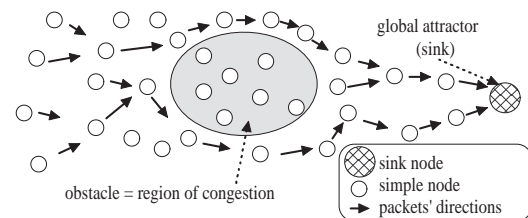


Fig. 1. Packet flock moving towards sink whilst avoiding 'obstacles'.

Each packet is modeled as a bird with dynamic position and direction updates, which 'flies' over the network undergoing successive hop-by-hop transitions over the hosting sensor nodes. In order to make moving packets behave like a flock,

each packet interacts with neighboring packets on the basis of attraction and repulsion forces, and experiences a ‘gravitational’ force in the direction of the sink (global attractor). In the proposed Flock-CC approach packets are (a) repelled from neighboring packets located on nodes experiencing high queue loading (crowded nodes), (b) attracted to neighboring packets located on nodes experiencing low wireless channel contention, (c) aligned with neighboring packets, using biased preference to packets located on nodes closer to the global attractor (i.e. the sink node), and (d) experience some perturbation that may help the packets to pick a random route (i.e. trading exploration versus exploitation). All these forces are incorporated into the mathematical model presented below.

A packet  $i$  and its hosting node  $n \in \{1, \dots, N\}$  are taken as points of reference in order to define and discuss sink direction discovery, the field of view, repulsion and attraction zones, and traffic management by means of a desirability function. All quantities defined herein are regularly sampled at discrete time intervals of  $T$  seconds at each sensor node and are broadcasted to all one-hop neighboring nodes (within transmission range).

The **direction of the sink** can be deduced by the hop distance variable,  $h_n(k)$ , indicating the number of hops between node  $n$  and the sink at the  $k$ th sampling period. Nodes located closer to the sink have smaller hop distance values and should be chosen with higher probability as next hop hosting nodes.

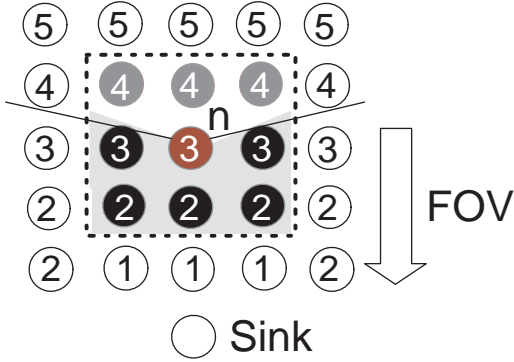


Fig. 2. The dashed square involves the transmission range of node  $n$ . The field of view (FoV) of packet  $i$  is illustrated by the grey shaded area. The number on each node indicates the hop distance from the sink.

Motivated by the limited visual field of birds, packet  $i$  does not ‘see’ all packets located on all nodes in the transmission range of the hosting node  $n$ , but only a fraction of these packets. In order for the flock to achieve orientation to the global target, the **field of view (FoV)** of each packet should cover the area in the direction of the sink. In the proposed approach, the FoV extends forward in the direction of decreasing hop distance towards the sink. In Fig. 2, the FoV of a packet  $i$  is represented by the grey shaded area inside the dashed square box, which includes only nodes with smaller hop distance or equal hop distance to the sink (compared with the hosting node  $n$ ’s hop distance). The expected number of nodes in the FoV of packet  $i$  is denoted by  $M$ ,  $M \leq N$ .

The field of view incorporates both the repulsion and the attraction zones, having repulsive and attractive forces exercised by packets located on each node  $m$ ,  $m \in \{1, \dots, M\}$  within the FoV (e.g. black shaded nodes of Fig. 2). The zone of repulsion (ZoR) is related to the queue of each node  $m$ , and the zone of attraction (ZoA) to the wireless channel in the vicinity of each node  $m$ .

Further to the discussion in Section II, the normalized queue occupancy (node loading) and the normalized wireless channel loading are adopted as good measures of the repulsion and attraction forces. The normalized node loading indicator  $p_m$  at node  $m$  is given by

$$p_m(k) = \begin{cases} 0, & \text{if } P_m^{in}(k) = 0, \\ & \text{and } P_m^{out}(k) = 0, \\ & \text{and } q_m(k^-) = 0; \\ \frac{P_m^{in}(k) + q_m(k^-) - P_m^{out}(k)}{P_m^{in}(k) + q_m(k^-)}, & \text{otherwise.} \end{cases} \quad (1)$$

where  $P_m^{in}(k)$  is the number of incoming packets,  $P_m^{out}(k)$  is the number of successful outgoing packets at the end of the  $k$ th period, and  $q_m(k^-)$  is the queue size at the beginning of the  $k$ th period at node  $m$ . More detailed information is given in [2]. When  $p_m(k) \rightarrow 0$ , both the number of packet drops due to buffer overflows at node  $m$  is close to 0 and the queue is empty or nearly empty. On the other hand, as  $p_m(k) \rightarrow 1$ , node  $m$  is considered congested due to either a high number of packet drops, or high queue occupancy. The parameter  $p_m(k)$  represents the repulsion force exercised on packet  $i$  by packets traversing the queue (ZoR) of each node  $m$  at the  $k$ th period.

The wireless channel quality can be evaluated using information collected from the MAC protocol (this study considers CSMA-like MAC protocols, e.g. IEEE 802.11) in terms of the normalized wireless channel loading at a node  $m$  which is denoted by:

$$r_m(k) = \begin{cases} 1 & \text{if retransmits} = 0 \text{ and } P_m^{out}(k) = 0; \\ \frac{P_m^{out}(k)}{P_m^{out*}(k)} & \text{otherwise.} \end{cases} \quad (2)$$

where  $P_m^{out*}(k)$  is the total number of all packet transmission attempts at node  $m$  during sampling period  $k$ , where  $P_m^{out*}(k) = P_m^{out}(k) + \text{retransmits}$  within that period. When  $r_m(k) \rightarrow 1$ , the channel is not congested and a large percentage of packets are successfully transmitted (few packet retransmissions are observed). As  $r_m(k) \rightarrow 0$ , the channel is congested and a small number of packets are successfully transmitted, often after a large number of retransmissions. The parameter  $r_m(k)$  represents the attraction force exercised on packet  $i$  by packets successfully transmitted through the wireless channel (ZoA), from each node  $m$ .

The **attraction and repulsion** forces are captured through a desirability function, which is supplemented by the other two properties of flock behavior, global attractiveness to the sink and randomness. Each hosting node evaluates the next hop node for each one of its packets based on an  $M$ -dimensional desirability vector,  $\vec{D}(k)$ . Each element,  $D_m(k)$ , of the vector  $\vec{D}(k)$  represents the desirability for each node

$m$ . The desirability  $D_m(k)$  for every node  $m$  is evaluated once in each sampling period  $k$  and is used for each packet sent within this period. It is given by:

$$D_m(k) = \alpha \cdot r_m(k) + (1 - \alpha) \cdot (1 - p_m(k)), \quad (3)$$

where the parameter  $\alpha$ ,  $0 \leq \alpha \leq 1$ , regulates the influence of parameters  $r_m(k)$  and  $p_m(k)$ .  $D_m(k)$  measures the tendency of packets to move towards node  $m$ .

If the **attractiveness to the sink** is ignored, a packet may not choose to move towards nodes placed closer to the sink. It is thus possible to get caught in a loop between a set of neighboring nodes. A natural way to address global attractiveness to the sink is to insist that only nodes in the FoV, strictly closer to the sink than the hosting node  $n$ , are considered when choosing the new hosting node. This solution excludes consideration of other nodes which are not necessarily on the direct path, but may have higher desirability, and makes paths towards the sink ‘too narrow’, thus aiding contention and node loading. In Flock-CC, packets are allowed to be forwarded even to nodes in the FoV that are placed at equal hop distance from the sink as the hosting node  $n$ , but some bias is applied against such a choice by discounting the desirability of equal hop distance nodes over the nodes that are closer to the sink. The discount factor,  $d_{im}(t)$ , is defined as:

$$d_{im}(t) = \begin{cases} 1 & \text{if } h_n(k) > h_m(k), \\ e & \text{if } h_n(k) = h_m(k). \end{cases} \quad (4)$$

where  $h_n(k)$  is the hop distance of node  $n$ , and  $h_m(k)$  is the hop distance of every node  $m$  at the  $k$  th sampling period. More specifically,  $d_{im}(k)$  is set equal to 1 for all nodes  $m$  in the FoV that are closer to the sink than the hosting node  $n$ , and equal to some constant  $e$ ,  $0 \leq e \leq 1$ , for all nodes  $m$  in the FoV at equal distance from the sink.

**Randomness** is experienced by introducing some noise in the desirability function. This noise (perturbation) is achieved by multiplying the desirability of a node by some coefficient drawn randomly from a Gaussian distribution with mean 1 and variance  $v$ . The variance  $v$  is a parameter of Flock-CC that is fixed within each experiment. Let  $g$  be a random variable that follows the Gaussian distribution,  $g \sim N(1, v)$ .

It can be deduced that nodes placed at equal hop distance from the sink can be selected if the noise perturbation is sufficiently large to cover the bias against these nodes, that is introduced by multiplying their desirability by  $e$ . The probability  $1 - e$  with which this bias is covered depends on the standard deviation  $\sqrt{v}$  of the Gaussian distribution. It makes sense to define  $v$  (and thus  $\sqrt{v}$ ) not entirely independently of  $1 - e$ , but as a linear function of  $1 - e$ . Thus, let  $v = c \cdot (1 - e)^2$  (and thus  $\sqrt{v}$  is linear in  $1 - e$ ). The value of  $c$  is varied in the experiments (and then  $v$  is computed), instead of varying  $v$  directly.

Following the discussion above, the *adjusted* desirability of packet  $i$  for node  $m$  is defined as:

$$D'_{im}(t) = g \cdot d_{im}(t) \cdot D_m(k). \quad (5)$$

After the evaluation of the adjusted desirability vector, the node  $m^*$  with the maximum adjusted desirability,

$$m^* = \operatorname{argmax}_m \{\vec{D}'_i(t)\} \quad (6)$$

is chosen as the new hosting node of packet  $i$ .

**Design parameters**  $\alpha$ ,  $e$ , and  $c$  need to be carefully selected.  $\alpha$  represents a tradeoff between the attraction and repulsion forces,  $e$  represents the bias away from direct paths, and  $c$  trades off exploration versus exploitation. In this paper, a simulation approach is adopted.

#### IV. PERFORMANCE EVALUATION

This section evaluates the performance of the Flock-CC approach through simulation studies conducted using the ns-2 network simulator. In accordance with [4], the optimal combination of the design parameters values achieving high packet delivery ratio (PDR), low end-to-end delay (EED), and low energy tax in a uniform grid topology was  $\alpha = 0.5$ ,  $e = 0.5$  and  $c = 0.25$ . The applicability of these values in random topologies is investigated below.

The evaluation topology consists of 400 homogeneous nodes deployed in a uniform random manner over an area of  $300 \times 300 m^2$ . The evaluation scenario involved the activation of 10 nodes placed in the same neighborhood, 7 hops away from the sink. In practise, it is quite common to have nodes closely located to each other being activated almost at the same time when an external stimulus (event) is detected. In the scenario under study, each active node generated constant bit rate traffic at the rates of either 25, or 35, or 45 pkts/s (all nodes at the same rate, different for each scenario) when triggered by an event. These three cases can be considered as slightly congested, congested, and heavily congested, respectively. The buffer capacity of each node was set to 35 KB. The sampling period  $T$  was set to 1 s. The selection of 1 s is guided by the desire to maintain responsiveness to changes in the network state and to avoid overwhelming the network with control packets. The CSMA-based IEEE 802.11 MAC protocol with 2 Mbps transmission rate was used.

##### A. Selection of design parameters $\alpha$ , $e$ and $c$

Each scenario, concerning different combinations of  $\alpha$ ,  $e$  and  $c$  values, was executed 10 times and the mean values of the metrics are presented below. The mean values are supplemented with 95% confidence intervals. Initially, active nodes were considered to generate traffic at the rate of 35 pkts/s.

Fig. 3 illustrates the impact of  $\alpha$ ,  $e$  and  $c$  on packet delivery ratio (PDR). As shown in Fig. 3, PDR deteriorated for  $e \geq 0.75$ , because packets were caught in loops between neighboring nodes, causing excessive packet loss attributed to both wireless channel collisions and buffer overflows (see Fig. 4). As can be seen, a higher PDR was achieved when  $\alpha = 0.5$ ,  $e = 0.5$  and  $c = 0.25$  or  $c = 0.5$ . When  $c = 0$ , the non-randomizing selection of new hosting nodes did not allow packets to exploit all the available paths to the sink causing a high number of buffer overflows (see Fig. 4). On

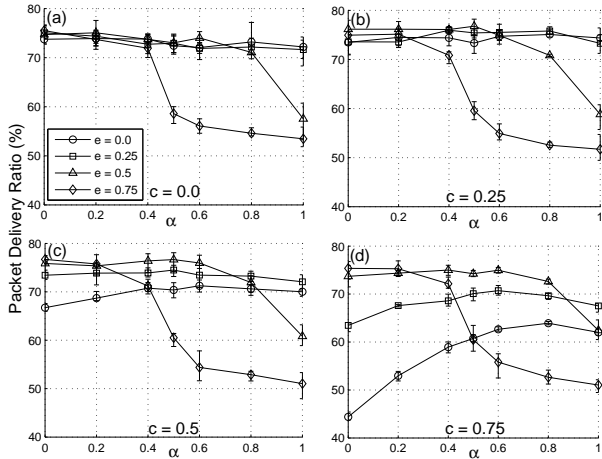


Fig. 3. Packet Delivery Ratio (35 pkts/s).

the other hand, large values of  $c$  (high randomization) resulted in low PDR values, because packets were trapped in loops.

The good compromise choice of  $\alpha = 0.5$  allows for a balanced influence of parameters  $r_m$  and  $p_m$  on the desirability function of Eq. 3. When  $\alpha < 0.5$ , the selection of a new hosting node is governed by the queue node loading indicator  $p_m$  without taking into account the wireless channel conditions in the vicinity of each potential hosting node. On the other hand, an increase of  $\alpha$  beyond 0.5 minimizes the influence of  $p_m$  on the desirability function. Thus, the repulsion forces from nodes with high loading decay, and packets are not prevented from moving towards ‘crowded’ nodes (causing high buffer overflows). Further evaluation results showed that the same behavior was exhibited for both lower and higher traffic load at the rates of 25 and 45 pkts/s respectively.

Fig. 4 displays the number of packets lost due to collisions

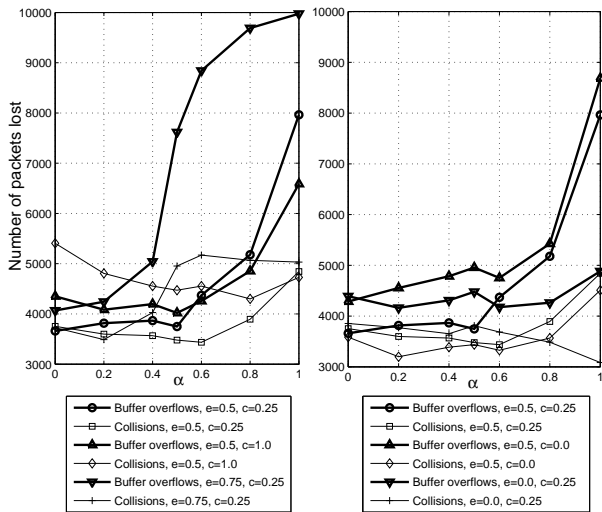


Fig. 4. Number of packet lost due to collisions and buffer overflows (35 pkts/s).

and buffer overflows when active nodes send at 35 pkts/s for different combinations of parameters  $\alpha$ ,  $e$  and  $c$ . It can be observed that for the majority of combinations of  $e$  and  $c$  values, the number of buffer overflows was greater than the number of collisions. In networks with random node deployment, there might not exist a large number of available paths to the sink, thus packets are traversing the network through a small number of alternative paths. Therefore, the buffers of nodes involved in these paths are frequently overwhelmed by packets leading to buffer overflows. It can be observed that the smallest number of packets lost (cumulatively due to collisions and buffer overflows) was achieved for  $\alpha = 0.5$ ,  $e = 0.5$  and  $c = 0.25$ . This combination of  $e$  and  $c$  parameters was compared against extreme values of  $e$  and  $c$ , keeping one of these parameters to its best case value. Remarkably high packet losses occurred for  $e = 0.75$  (collisions + buffer overflows) due to the looping behavior of packets inside the network as shown in Fig. 4(a). On the other hand, low packet losses were observed for  $e = 0$  in Fig. 4(b) because the narrow field of view disabled high packet spreading, and thus packet looping. Also, a high number of buffer overflows was observed with an increase of  $\alpha$  (beyond a certain value, different for each scenario, but mostly greater than 0.5) for the reason described above.

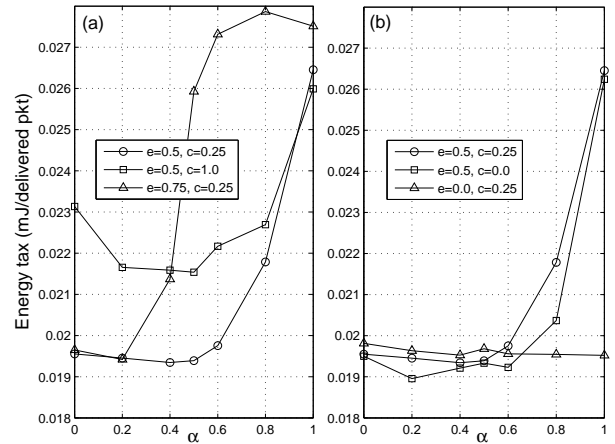


Fig. 5. Energy tax measured in mJoules per delivered packet (35 pkts/s).

Fig. 5 presents the energy tax paid per delivered packet for certain combinations of parameters  $\alpha$ ,  $e$  and  $c$ . It can be observed that the lowest energy tax was paid for the combination  $\alpha = 0.2$ ,  $e = 0.5$  and  $c = 0$  but this was at the expense of lower PDR. As shown in Fig. 4(b), the low energy tax was attributed to the low number of collisions, and thus to the low number of retransmissions at the MAC layer. Also, low energy tax was paid for the combination  $\alpha = 0.5$ ,  $e = 0.5$  and  $c = 0.25$  which achieved good compromise in terms of PDR and EED. It is also apparent that a large amount of energy was consumed when  $e = 0.75$ ,  $c = 0.25$ ,  $\alpha > 0.2$  and  $e = 0.5$ ,  $\alpha > 0.6$  due to the vast number of retransmissions of packets that were lost due to buffer overflows (mostly) and collisions.

Based on all the experimental results presented thus far, a

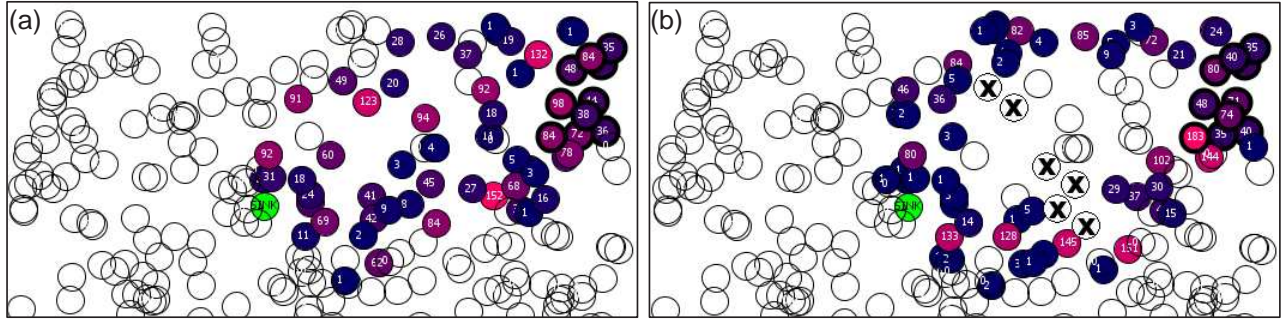


Fig. 6. Emergent behavior of moving packets at the presence of failures: (a) Before failures, (b) After failures. A small region of the network involving packet activity is illustrated.

good compromise combination of the design parameters values achieving a good behavior in terms of high PDR and low EED in the scenario under study, was  $a = 0.5$ ,  $e = 0.5$  and  $c = 0.25$ . This combination also achieved low energy consumption.

### B. Emergent behavior

The emergent behavior of the collective motion of packet flocks is investigated below. The sink node is depicted in the middle of Fig. 7 (pointed out by a black arrow), while active nodes are highlighted by bold circles in the upper right corner of the network. The values of  $\alpha$ ,  $e$ ,  $c$  and  $T$  were set to 0.5, 0.5, 0.25 and 1 s respectively.

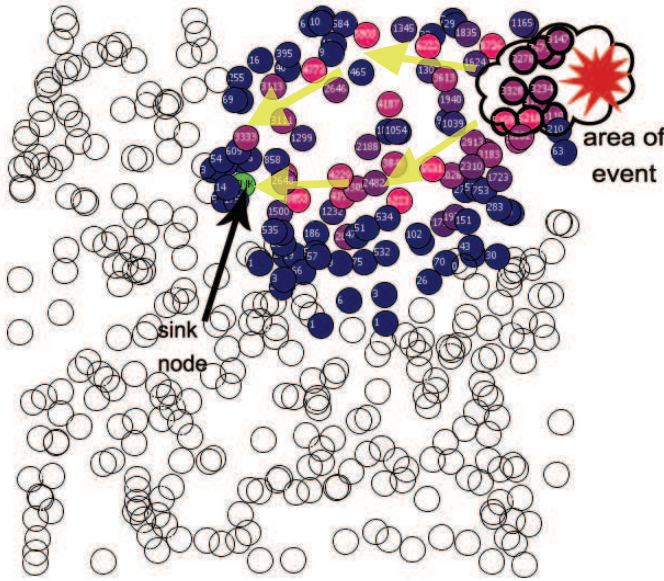


Fig. 7. Emergent behavior of moving packets towards the sink. The intensity of the number of packets arriving at each node is indicated by darker colors and the actual number is indicated inside every node.

As can be seen, due to the flocking behavior, packets were spread in the network exploiting all available paths whilst moving towards the sink. There were two shortest paths to the sink (indicated by the two arrows in Fig. 7) which were traversed by the majority of the packets. Furthermore, the rest

of the packets, which were repelled by packets located on the highly crowded nodes (as dictated by the bird flocking behavior), followed alternative paths (dark shaded nodes).

### C. Robustness to failures

Sensor nodes are prone to failures, mainly due to fabrication process problems, environmental factors (disasters), enemy attacks, and battery power depletion. The Flock-CC approach exhibits robustness against node failures due to the inherent tendency of individuals to follow other flockmates that manoeuvre to avoid obstacles (e.g. congestion regions, failing nodes).

Fig. 6 shows two network snapshots, before and after node failures. It is apparent that the Flock-CC approach displayed outstanding flocking behavior in the presence of numerous node failures, and exemplified all of the characteristics of a bird flock in terms of obstacle avoidance and manoeuvring around the zone of dead nodes. Results showed that Flock-CC provided graceful performance degradation when node failures occurred exhibiting a slight decrease in packet delivery ratio and a small increase in end-to-end delay.

### D. Comparative evaluations

The proposed Flock-CC approach (that incorporates both routing and congestion control capabilities) was compared with (a) a conventional congestion-free multi-path routing protocol based on shortest paths, (b) a typical congestion-aware routing protocol that routes packets over multiple paths, choosing each time the least congested node in terms of queue length, and (c) AODV [11], a well known single-path routing protocol for ad-hoc networks.

The Flock-CC parameters  $\alpha$ ,  $e$  and  $c$  were set to 0.5, 0.5 and 0.25 respectively. Fig. 8 shows that the Flock-CC approach clearly outperformed all other approaches in terms of both PDR and EED, for all transmission rates. From the perspective of PDR, the Flock-CC approach delivered around 16% more packets than the congestion-free protocol under low and medium loads, and around 10% more packets under high loads. Similarly, the Flock-CC approach achieved 5–7% higher PDR compared with the congestion-aware routing protocol. Flock-CC also outperformed AODV by 38–60%.

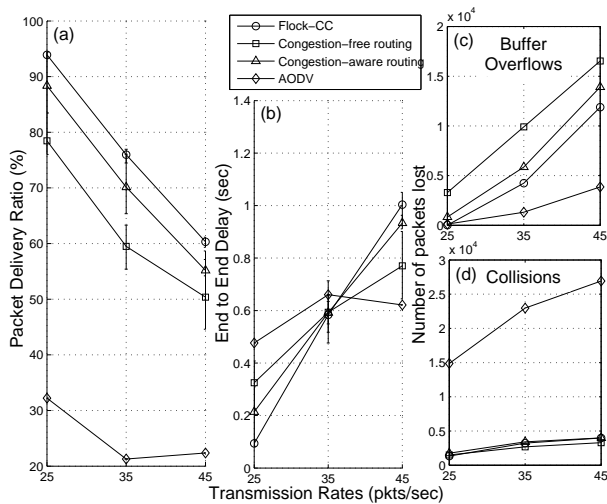


Fig. 8. Comparative experiments.

For the congestion-free protocol, packets were sent over the shortest path, while the congestion-aware protocol allows for packet spreading if queues were filling up. This behavior is illustrated in Figs. 8(c) and (d). A remarkable observation is that the Flock-CC approach exhibited low buffer overflows compared to the congestion-free and congestion-aware protocols due to its traffic spreading ability. AODV achieved minimal buffer overflows something that is explained by looking at Fig. 8(d). AODV suffered heavily from collisions, while the problem worsened with the increase of traffic load. This problem was attributed to the high number of broadcasted control messages that led to wireless channel capacity saturation. As a result, buffers were rarely filled up. The other three protocols exhibited significantly lower number of collisions.

Fig. 8(b) shows that the Flock-CC approach exhibited the lowest EED among the other protocols for every transmission rate, because traffic spreading prevented augmented buffer occupancies which contribute to larger queuing delays. Note that only packets successfully received at the sink were involved in EED evaluation. In line with this statement, AODV exhibited low EED in high load conditions, since the majority of packets were lost.

## V. CONCLUSION

In this paper, the Flock-CC mechanism was evaluated on a random topology. Performance evaluations showed that the Flock-CC mechanism was able to both alleviate congestion (using packet spreading motivated by the bird flocking behavior) and minimize energy tax. Also, Flock-CC showed robustness against failing nodes, and outperformed congestion-aware and congestion-unaware routing approaches in terms of PDR, EED and energy tax. The future work will provide more comparative evaluations and investigation of the influence of the sampling period  $T$ .

## ACKNOWLEDGMENT

This work is supported in part by the GINSENG project funded by the 7<sup>th</sup> Framework Programme under Grant No. ICT-224282 and the MiND2C project funded by the Research Promotion Foundation of Cyprus under Grant No. TPE/EPIKOI/0308(BE)/03.

## REFERENCES

- [1] P. Antoniou, A. Pitsillides, T. Blackwell and A. Engelbrecht, Employing the Flocking Behavior of Birds for Controlling Congestion in Autonomous Decentralized Networks, IEEE CEC2009, Norway.
- [2] P. Antoniou, A. Pitsillides, A. Engelbrecht and T. Blackwell, A Swarm Intelligence Congestion Control Approach for Autonomous Decentralized Communication Networks, to Appear in Applied Swarm Intelligence, edited by Engelbrecht A. and Middendorf M, Springer Series in Studies in Computational Intelligence.
- [3] P. Antoniou, A. Pitsillides, A. Engelbrecht, T. Blackwell and L. Michael, Congestion Control in Wireless Sensor Networks Based on the Bird Flocking Behavior, 4th IFIP IWSOS 2009, Switzerland.
- [4] M. Loizou, Mimicking Nature in Designing Robust Congestion Control Mechanism in Sensor Networks (in Greek), Undergraduate thesis (advisor: A. Pitsillides), Department of Computer Science, University of Cyprus, 2010. This document can be accessed online at <http://www.mind2c.cs.ucy.ac.cy/docs/Marinathesis.pdf>
- [5] C. Wan, S. Eisenman and A. Campbell, CODA: Congestion Detection and Avoidance in Sensor Networks, 1st Int. Conf. on Embedded Net. Sensor Systems, 2003, pp. 266-279.
- [6] B. Hull, K. Jamieson and H. Balakrishnan, Mitigating Congestion in Wireless Sensor Networks, 2nd Int. Conf. on Embedded Net. Sensor Systems, 2004, pp. 134-147.
- [7] M. C. Vuran, V. C. Gungor and O. B. Akan, On the Interdependence of Congestion and Contention in WSNs, ICST SenMetrics, 2005.
- [8] T. He, F. Ren, C. Lin and S. Das, Alleviating Congestion Using Traffic-Aware Dynamic Routing in Wireless Sensor Networks, 5th Annual IEEE Comm. Soc. Conf. on Sensor, Mesh and Ad Hoc Comm. and Net., 2008. SECON '08.
- [9] K. Karenos, V. Kalogeraki and S. V. Krishnamurthy, Cluster-based Congestion Control for Sensor Networks, ACM Transactions on Sensor Networks, Vol. 4, No. 1, January 2008.
- [10] C.-Y. Wan, S. B. Eisenman, A. T. Campbell, and J. Crowcroft, Siphon: Overload traffic management using multi-radio virtual sinks in sensor networks, ACM SenSys, Nov. 2005.
- [11] C. E. Perkins, Ad Hoc On Demand Distance Vector (AODV) Routing, RFC 3561, 1997.